

Cite this: *Dalton Trans.*, 2013, **42**, 9645

Received 8th March 2013,
Accepted 4th May 2013

DOI: 10.1039/c3dt50653c

www.rsc.org/dalton

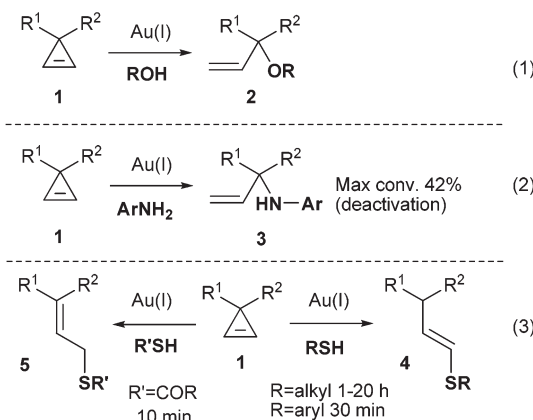
1 Introduction

In less than a decade, homogenous gold catalysis has undergone a transformation from rarity to an incredibly active and rapidly evolving field of research.¹ Its popularity is partly result of the excellent selectivity and efficiency of gold catalysts as π -Lewis acids for activating C–C π bonds, and also the ability to tune gold catalysts in order to vary the reactivity and selectivity of the reactions.¹ One of the research efforts within our group is to explore the diverse chemistry of gold-catalysed reactions with cyclopropenes,^{2,3} alenes⁴ and allylic alcohols.⁵ Within this context, we have used alcohols,^{2a,b,4,5} amines^{2f} and thiols^{2f} as nucleophiles in gold-catalysed reactions, and have observed that the presence of these nucleophiles can dramatically alter the reactivity as well as selectivity of the gold catalysts. For example, we have previously observed that although gold(i)-catalysed reactions can work very well with alcohol nucleophiles^{1f} (Scheme 1, eqn (1)),^{2a,b,4a} the equivalent reaction of anilines with cyclopropenes do not proceed to completion (Scheme 1, eqn (2)),^{2f} presumably due to deactivation of the catalyst by the *N*-nucleophile. On the other hand, despite the initial assumption that *S*-nucleophiles would fare worse than *N*-nucleophiles (as they are known strong coordinators to gold),⁶ reactions with thiols *do* proceed to completion.⁷ However, reactions are clearly slower with more nucleophilic *S*-nucleophiles (progressively slower from thioacid→thiophenol→alkyl thiols, Scheme 1, eqn (3)).^{2f} Furthermore, functionalities such as furans^{2c} and alcohols,^{2a,b} which usually react

Deactivation of gold(i) catalysts in the presence of thiols and amines – characterisation and catalyst

Paul C. Young, Samantha L. J. Green, Georgina M. Rosair and Ai-Lan Lee*

Thiols and amines, which are common heteroatom nucleophiles in gold-catalysed reactions, are known to dampen the reactivity of gold catalysts. In this article, the identity and activity of gold(i) catalysts in the presence of thiols and amines is investigated. In the presence of thioacid, thiophenol and thiol, digold with bridging thiolate complexes $[\{Au(L)\}_2(\mu-SR)][SbF_6]$ are formed and have been fully characterised by NMR and X-ray crystallography. In the presence of amines and anilines, complexes $[LAu-NH_2R][SbF_6]$ are formed instead. All new isolated gold complexes were investigated for their catalytic activity in order to compare the level of deactivation in each species.



Scheme 1 Previous work: gold(i) catalysed reactions of cyclopropenes with (1) alcohols; (2) anilines; (3) thiols.

with cyclopropenes within minutes under gold(i)-catalysis, are no longer reactive in the presence of thiols.^{2f}

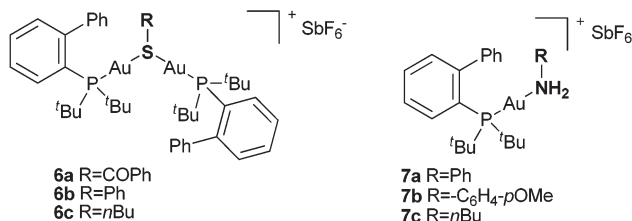
In order to explain these observations, we were keen to elucidate the structure and activity of the actual gold(i) species involved in these reactions.^{8,9} So far, not much effort has been made to isolate, characterise¹⁰ and investigate the catalytic properties of these species. Nevertheless, heteroatom nucleophiles such as RSH and RNH₂ are commonly used in gold-catalysed reactions,^{1a,d} so a better understanding of the nature and activity of gold(i) catalysts in the presence of these nucleophiles will be invaluable if we are to better understand the mechanisms of gold-catalysed reactions.¹¹

In a recent publication describing the gold(i)-catalysed reactions of thiols with cyclopropenes, we briefly disclosed that $[\{Au(L)\}_2(\mu-SR)][SbF_6]$ species are likely to be the thiol-deactivated complexes formed in the reaction.^{2f,12} In this article, we present our full investigations into the nature of the gold-

Institute of Chemical Sciences, Heriot-Watt University, Edinburgh, EH14 4AS, United Kingdom. E-mail: A.Lee@hw.ac.uk; Tel: +44 (0)131 4518030

† Electronic supplementary information (ESI) available: ¹H, ¹³C and ³¹P NMR spectra of all new compounds. CCDC 914704–914708. For ESI and crystallographic data in CIF or other electronic format see DOI: 10.1039/c3dt50653c





Scheme 2 Characterised deactivated gold(I) complexes 6a-c and 7a-c.

species formed in the presence of thiols, and compare these with species formed in the presence of amines. Solution state NMR studies are presented, along with the isolation and characterisation of the thiol-deactivated species $[\text{Au}(\text{L})_2(\mu\text{-SR})]\text{[SbF}_6]$ 6a-c and amine-deactivated species $[\text{LAu-NH}_2\text{R}]\text{[SbF}_6]$ 7a-c by NMR spectroscopy and X-ray crystallography (Scheme 2). Complexes of type $[\text{Au}(\text{L})_2(\mu\text{-SR})]\text{[SbF}_6]$ and $[\text{LAu-NH}_2\text{R}]\text{[SbF}_6]$ have never been studied in the context of catalysis, so 6a-c and 7a-c were investigated for their catalytic activity in an effort to compare the level of deactivation in each of these species.

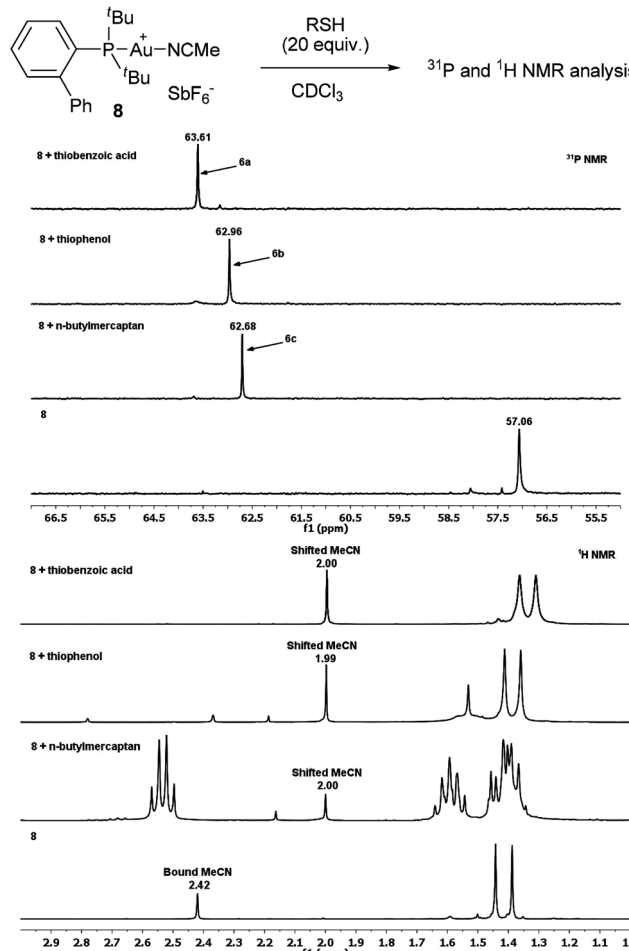
2 Results and discussion

2.1 Gold(I) catalyst with thiols, thiophenols and thioacids

Our investigations commenced with NMR studies of Echavarren catalyst¹³ 8 in the presence of sulfur nucleophiles RSH. Catalyst 8 is a commonly used, commercially available Au(I) catalyst and was chosen for our studies because it was previously found to have the best catalytic activity in the presence of thiols.^{2f} The second reason for using 8 is one of practicality: the displacement of the MeCN in the complex by an S-nucleophile can be clearly monitored by ¹H NMR spectroscopy, indicated by the appearance of unbound MeCN in the solution.

When catalyst 8 was subjected to 20 equiv. of an alkyl thiol, thiophenol or thiobenzoic acid (to replicate the ratio which would be present in a typical 5 mol% gold(I)-catalysed reaction), an almost instantaneous conversion to new complexes was observed by ³¹P NMR analysis (Fig. 1, top), backed up by the appearance of unbound MeCN in the ¹H NMR spectra (Fig. 1, bottom).

The analyses were repeated with 1:1 equiv. of 8 with the same thiols (see ESI†), and crystallisation by vapour diffusion method (CDCl₃-hexane) produced single crystals which were isolated and characterised by X-ray crystallography (Fig. 2). All three are revealed to be digold with bridging thiolate complexes¹⁴ $[\text{Au}(\text{L})_2(\mu\text{-SR})]\text{[SbF}_6]$ 6a, 6b and 6c, which are now fully characterised by X-ray crystallography, ¹H, ³¹P, ¹³C NMR, IR and HRMS (see section 4.2). Crystals of 6a-6c are all air-stable over a period of >3 months. There is no formal Au-Au bond,¹⁵ although the intramolecular Au-Au distance of 3.3987(3), 3.4066(4) and 3.4363(3) Å in 6a, 6b and 6c respectively may indicate weak aurophilic interactions (accepted range of aurophilic Au-Au distances ca. 2.85–3.50 Å).¹⁶ In addition, the aromatic ring from the ligand appears to be stabilising the

Fig. 1 ³¹P and ¹H NMR analysis of a 20:1 mixture of 8 and RSH.

Au centre through a weak Au(I)-arene interaction (Au–arene distances of 3.218/3.173, 3.212/3.183 and 3.218/3.204 Å for 6a, 6b and 6c respectively),¹⁶ an interaction which is also observed in the parent Echavarren catalyst 8.¹³ The ³¹P NMR shift moves more upfield the more nucleophilic the parent thiol RSH (63.61, 62.96, 62.68 for 6a, 6b and 6c respectively), consistent with a progressively more electron rich Au(I) centre.

A plausible mechanism for the formation of complexes 6a-c is shown in Scheme 3. Acetonitrile is displaced by RSH to form 9, followed by loss of H⁺ to form 10. Complex 10 is nucleophilic and reacts with 8 to form the observed digold complex 6. Evidence for the reversibility of this process is discussed in section 2.3.

2.2 Gold(I) catalyst with amines and anilines

Having evaluated the identity of the gold complexes in the presence of thiols, we next carried out a similar study with N-nucleophiles. With nBuNH₂, p-MeO-C₆H₄NH₂ (p-anisidine) and aniline, a clear shift in the ³¹P NMR peak is observed (Fig. 3), once again, accompanied by the appearance of unbound MeCN in the ¹H NMR spectra (see ESI†). The ³¹P NMR shift appears to move more upfield the better the parent



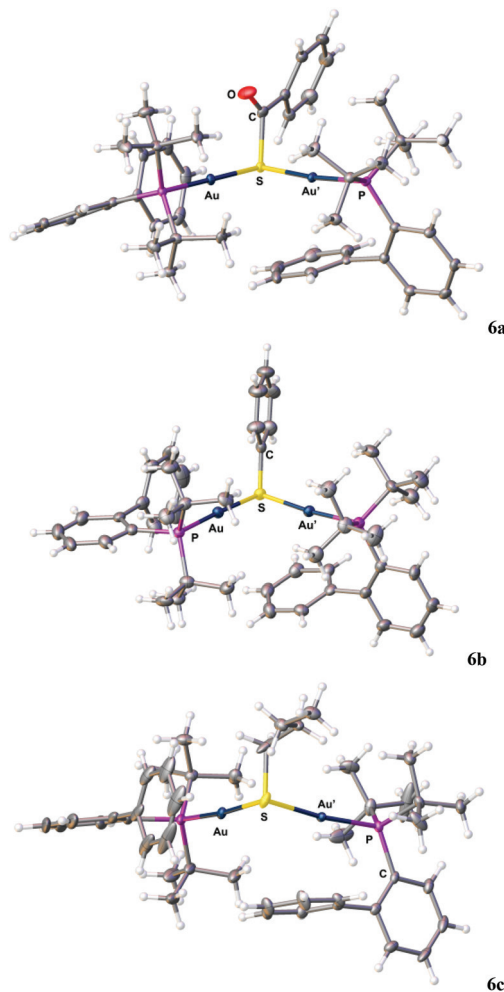
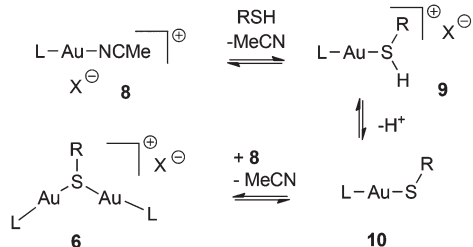


Fig. 2 X-ray structures of **6a**, **6b** and **6c**. SbF_6^- counterion is omitted for clarity and only one independent molecule shown for **6b**. **6a**: Au-S 2.3233(10), $\text{Au}'-\text{S}$ 2.3262(10) Å, $\text{Au-S-Au}'$ 93.94(3)°; **6b** Au-S 2.3190(16), Au-S 2.3362(16) Å, $\text{Au-S-Au}'$ 94.07(5)°; **6c** Au-S 2.3196(9), Au-S 2.3285(10) Å; $\text{Au-S-Au}'$ 95.34(3)°.



Scheme 3 Plausible mechanism for the formation of **6a-c**.

RNH_2 nucleophile, consistent with a progressively more electron rich $\text{Au}(\text{i})$ centre.

In order to characterise these species, single crystals were grown by vapour diffusion (CDCl_3 -hexane). In stark contrast to the digold species with thiols, single crystal X-ray crystallography reveals monogold $[\text{LAu-NH}_2\text{R}][\text{SbF}_6]$ species **7a**, **7b** and **7c** (Fig. 4). These species are more than likely to be the cause of

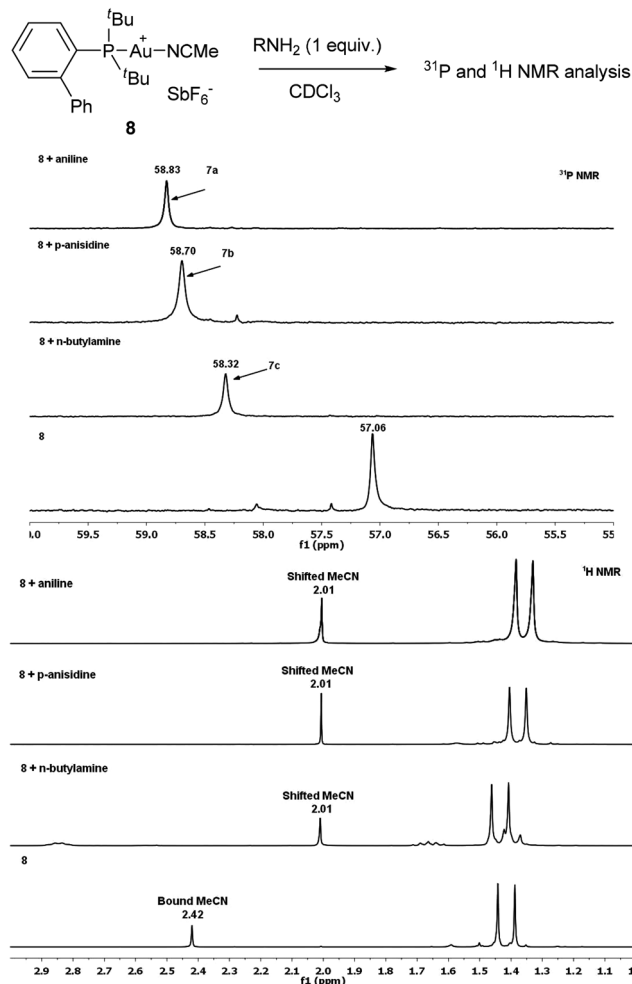


Fig. 3 ^{31}P and ^1H NMR analysis of a 1:1 mixture of **8** and RNH_2 .

dampening of reactivity in some gold(i)-catalysed reactions with amines and anilines (e.g. eqn (2), Scheme 1).¹⁷ The intermolecular Au-Au distances are 7.5686(4), 8.1290(3) and 7.6009(4) Å respectively for **7a**, **7b** and **7c**, showing that there are no significant Au-Au interactions. Weak Au-arene stabilisation of the Au centre by the ligand is once again evident in all of these structures (Au-arene distances of 3.154, 3.162 and 3.172 Å in **7a**, **7b** and **7c** respectively). This interaction is thought to render extra stability to the gold complexes in this study, and allows them to be stable (e.g. **7c** is air stable >6 months upon standing on the bench) and isolable for characterisation. In contrast, subsequent attempts to grow the corresponding NHC (IPr) versions of these complexes in the same manner led to decomposition.

While amines and anilines clearly react with the gold catalyst to form $[\text{LAu-NH}_2\text{R}][\text{SbF}_6]$, the less nucleophilic amide (PhCONH_2) and protected amines BocNH_2 and TsNH_2 do not show the same reactivity. When a 1:1 mix of catalyst **8** and these N -nucleophiles are monitored by NMR, no displacement of MeCN is seen in the ^1H NMR spectra, and no appreciable shift in the ^{31}P NMR is observed. While this observation does not rule out the formation of small amounts of $[\text{LAu-NH}_2\text{R}]$ -

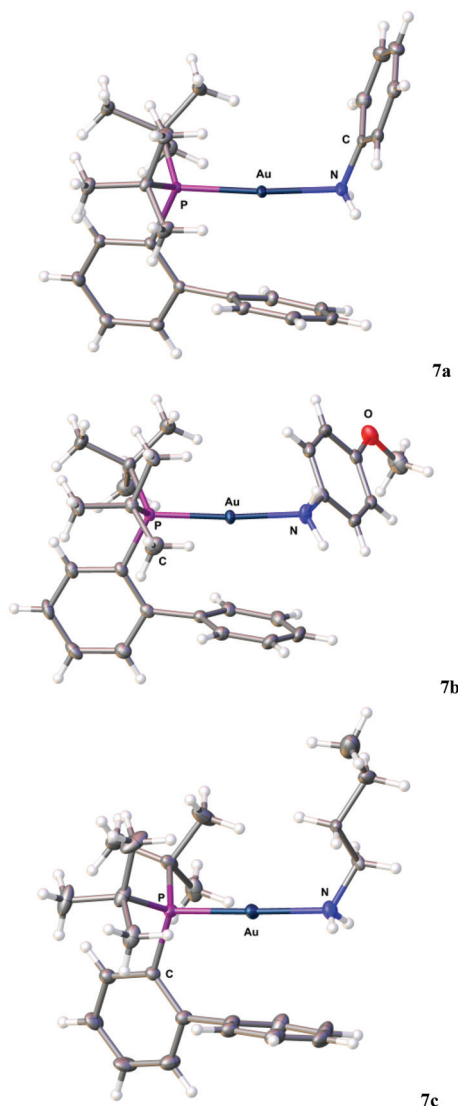
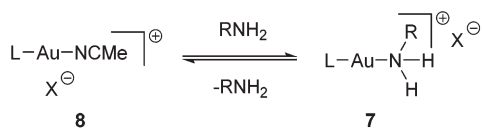


Fig. 4 X-ray structures of **7a**, **7b** and **7c**. SbF_6^- counterion is omitted for clarity. **7a**: Au–N 2.1197(17) Å, N–Au–P 172.28(6)°; **7b** Au–N 2.116(4) Å, N–Au–P 175.76(11)°; **7c** Au–N 2.097(2) Å, N–Au–P 175.22(8)°.



Scheme 4 Formation of complex **7**.

$[\text{SbF}_6^-]$ in solution, the equilibrium firmly lies towards **8** (in Scheme 4).¹⁸ This observation is as expected as it reflects the catalytic activity of gold(i) in the presence of *N*-nucleophiles: protected amines such as Boc- and Ts-amines are more commonly used nucleophiles.^{1a,d}

2.3 Catalytic studies with **6a–c** and **7a–c**

Having established, isolated and characterised the gold(i) species in the presence of RSH and RNH_2 (**6a–c** and **7a–c**

respectively), we set out to study the catalytic activity of these species. Complexes of type $[\{\text{Au}(\text{L})\}_2(\mu-\text{SR})][\text{SbF}_6^-]$ and $[\text{LAu}-\text{NH}_2\text{R}][\text{SbF}_6^-]$ have never been studied in the context of catalysis, so it will be useful to know whether these complexes are completely inactive or whether they can competently release active catalyst *in situ*. For example, in related work, formation of carbon bridged digold species have been shown to be inhibitory to catalysis as they are in competition with the product yielding protodeauration step.¹⁹ Related $[\{\text{Au}(\text{L})\}_2(\mu-\text{OH})][\text{X}]$ complexes have also been reported and utilised as active catalysts.²⁰ In addition, we were also keen to investigate the degree of deactivation in **6a–c** and **7a–c** relative to each other.

Firstly, $[\{\text{Au}(\text{L})\}_2(\mu-\text{SR})][\text{SbF}_6^-]$ was investigated in a reaction with RSH as a nucleophile, in order to ascertain whether it could be the actual catalytically active species in these reactions. When complex **6b** was used as a catalyst in a reaction of a cyclopropene^{21,22} with thiophenol,^{2f} the production of the gold(i) catalysed product **12** is nowhere near as good as with the parent catalyst **8** (Table 1, entry 3 vs. 1). Instead, the background (non gold(i)-catalysed) addition reaction to form cyclopropane **13** dominates. This initially suggests that **6b** is most likely *not* the active catalyst in the reaction shown in entry 1, Table 1, and is instead a deactivation pathway in gold(i)-catalysed reactions with thiols.

However, this result was initially rather puzzling as the procedure in entry 1 involves pre-mixing catalyst **8** with PhSH in CH_2Cl_2 *before* addition to cyclopropene substrate **11**: this forms **6b** *in situ* almost instantaneously (see section 2.1). One difference between using isolated **6b** (entry 3) and **6b** made *in situ* from **8** (entry 1) is the presence of H^+ , released upon formation of **6b** from **8** (Scheme 3).²³ If the formation of **6** from **8** is indeed reversible, then the presence of H^+ may allow for more active catalyst to be in solution for catalysis, whereas the absence of residual H^+ (entry 3) causes the equilibrium to be towards inactive **6**. Indeed, when **6b** is used *with added* H^+ , the gold(i)-catalysed product **12** is once again the major product (entry 4). A control reaction using Brønsted acid alone (entry 5)

Table 1 Comparison of the reaction of cyclopropene **11** with thiophenol in the presence of **8** and **6b**; and control reactions

Entry	Catalyst	mol%	12 : 13 ^a
1 ^b	8	5	12 only
2	No catalyst	N/A	13 only
3	6b	2.5	1 : 20
4	6b + HOTf	2.5	2 : 1
5	HOTf	2.5	13 only

^a Determined by ^1H NMR analysis of crude reaction mixture. ^b **8** is pre-mixed with PhSH in CH_2Cl_2 before addition to **11**.

shows that the reaction to form **12** in entry 4 is gold(i)-catalysed.

Next, $[\text{LAu-NH}_2\text{R}][\text{SbF}_6]$ complex **7b** was investigated in a reaction where RNH_2 is a nucleophile. When complex **7b** was used as a catalyst in a reaction of a cyclopropene with *p*-anisidine, the conversion to **15** is 15% with **7b** compared to 27% using catalyst **8** (entries 1–2, Table 2). As expected, addition of acid does not improve the conversion to desired product (entry 3, Table 2 vs. entry 4, Table 1) as this time it does not affect the equilibrium between **8** and **7** (Scheme 4). ^{31}P NMR analysis of a 1:1:1 ratio of **8**:**7b**:*p*-anisidine in CD_2Cl_2 clearly shows immediate formation of **7b** *in situ*, which persists after 2 hours.

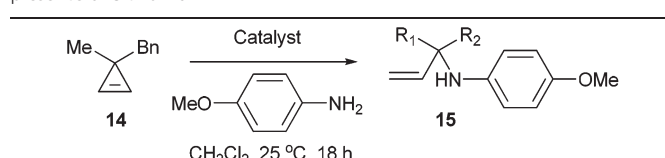
Finally, the gold(i)-catalysed reaction of alcohols with cyclopropenes (eqn (1), Scheme 1) was used to compare the catalytic activities (or rather, the amount of dampening of catalytic activity) of complexes **6a–c** and **7a–c**. We have previously shown that this reaction goes to full conversion with a variety of commercial gold(i) catalysts.^{2a,b} In comparison, complexes **6a–c** do not produce full conversions to product **16** (entries 1–3, Table 3). The conversions are moderate to low: 47%, 25% and <5% respectively for **6a**, **6b**, and **6c**. This observed trend neatly reflects the Lewis basicity of the original RSH thiol employed to form the complexes **6a–c**. The increasing Lewis

basicity going from thioacid→thiophenol→alkyl thiol to form **6a**, **6b**, and **6c** respectively is likely to push the equilibrium towards **6** (Scheme 3), resulting in a lower concentration of active catalyst in the reaction. Complexes **7a–c** show a similar trend (entries 4–6). The conversions, reflecting the catalytic activity, also decrease going from **7a**→**7b**→**7c**, reflecting the increasing Lewis basicity of the parent aniline→anisidine→amine.

3 Conclusions

In conclusion, we found that thiols deactivate Au(i) catalysts by forming digold with bridging thiolate complexes $[\{\text{Au(L)}_2\}(\mu\text{-SR})][\text{SbF}_6]$ (e.g. **6a–c**, which have now been fully characterised). These species are in equilibrium with the active gold catalysts (Scheme 3) and the presence of residual H^+ *in situ* is required for enough active catalyst to be in solution for catalysis, whereas the absence of residual H^+ causes the equilibrium to shift towards the inactive complex **6**. In addition, the more nucleophilic the parent thiol (RSH), the less active the resulting gold(i) complex, presumably because this pushes the equilibrium increasingly towards the inactive complex $[\{\text{Au(L)}_2\}(\mu\text{-SR})][\text{SbF}_6]$. In contrast, amines deactivate Au(i) catalysts by forming the monogold species $[\text{LAu-NH}_2\text{R}][\text{SbF}_6]$ (e.g. **7a–c**). The difference in behaviour between gold(i) complexes in thiols and amines is possibly due to the difference in acidity of the proton in **9** vs. **7**. We hope that these results shed some light on the identity as well as activity of gold(i) catalysts when thiols and amines are used as nucleophiles in gold(i)-catalysed reactions.

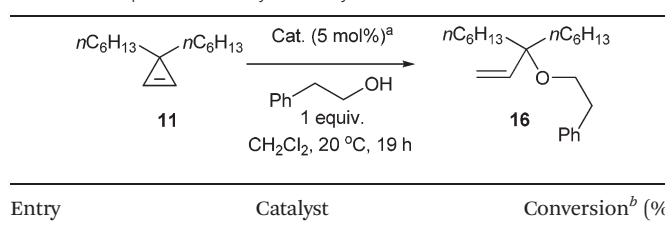
Table 2 Comparison of the reaction of cyclopropene **14** with *p*-anisidine in the presence of **8** and **7b**



Entry	Catalyst	mol%	Conversion ^a (%)
1	8	5	27
2	7b	5	15
3	7b + HOTf	5 + 5	13

^a Determined by ^1H NMR of crude reaction mixture.

Table 3 Comparison of catalytic activity of **6a–c** and **7a–c**



Entry	Catalyst	Conversion ^b (%)
1	6a	47
2	6b	25
3	6c	<5
4	7a	47
5	7b	43
6	7c	34

^a 5 mol% with respect to gold, i.e. 2.5 mol% for digold species **6a–c**.

^b Determined by ^1H NMR analysis of crude reaction mixture.

4 Experimental

4.1 General experimental section

All reactions were carried out in air without the need for pre-dried solvents, in order to replicate the reaction conditions in gold(i) catalysed reactions, which are typically carried out in air. ^1H NMR spectra were recorded on Bruker AV 300 and AV 400 spectrometers at 300 and 400 MHz respectively and referenced to residual solvent. ^{13}C NMR spectra were recorded using the same spectrometers at 75 and 100 MHz respectively. Chemical shifts (δ in ppm) were referenced to tetramethylsilane (TMS) or to residual solvent peaks (CDCl_3 at δ = 7.26). For ^{31}P NMR, chemical shifts were referenced against H_3PO_4 at δ 0 ppm. J values are given in Hz and s, d, dd, t, q and m abbreviations correspond to singlet, doublet, doublet of doublet, triplet, quartet and multiplet. Mass spectrometry data was acquired at the EPSRC UK National Mass Spectrometry Facility at Swansea University. Infrared spectra were obtained on Perkin-Elmer Spectrum 100 FT-IR Universal ATR Sampling Accessory, deposited neat or as a chloroform solution to a diamond/ZnSe plate. Elemental analyses were determined by the departmental service (HWU). Flash column chromatography was carried out using Matrix silica gel 60 from Fisher



Chemicals and TLC was performed using Merck silica gel 60 F254 precoated sheets and visualised by UV (254 nm) or stained by the use of aqueous acidic ceric ammonium molybdate. Petrol ether refers to petroleum ether (40–60 °C). Dichloromethane (DCM) was purchased from Fisher and used without further purification. All nucleophiles were purchased from Sigma-Aldrich or Acros, and used without further purification.

4.2 General experimental procedure for crystals 6a–c and 7a–c

Catalyst **8** and the nucleophile RSH or RNH₂ (1 equiv.) were added to an NMR tube, and dissolved in CDCl₃ (0.75 mL). ¹H and ³¹P NMR were obtained from the resulting crude mixture. The solution was then decanted into a vial, and crystals were grown by vapour diffusion from CDCl₃-hexane. The crystals were washed with hexane and dried under reduced pressure.

Compound 6a. Complex **6a** was obtained as yellow crystals (9.3 mg, 0.0068 mmol, 26%). M.p. 195 °C (decomposes). ¹H NMR (300 MHz, CDCl₃) δ 7.94–7.80 (m, 4H, Ar-H), 7.64–7.11 (m, 19H, Ar-H), 1.30 (d, *J* = 16.0, 36H, C(CH₃)₃); ¹³C NMR (100 MHz, CDCl₃) δ = 189.5 (C), 149.2 (d, *J*(¹³C–³¹P) = 13.5 Hz, C), 143.1 (d, *J*(¹³C–³¹P) = 6.8 Hz, C), 138.3 (C), 134.5 (d, *J*(¹³C–³¹P) = 11.8 Hz, CH), 133.9 (CH), 133.3 (CH) (d, *J*(¹³C–³¹P) = 7.7 Hz, CH), 131.4 (CH), 129.7 (CH), 129.4 (CH), 129.1 (d, *J*(¹³C–³¹P) = 16.1 Hz, CH), 128.9 (CH), 128.7 (CH), 128.3 (CH), 128.0 (CH), 127.8 (d, *J*(¹³C–³¹P) = 7.0 Hz, CH), 125.4 (d, *J*(¹³C–³¹P) = 45.0 Hz, C), 38.2 (d, *J*(¹³C–³¹P) = 23.8 Hz, C), 30.8 (d, *J*(¹³C–³¹P) = 6.7 Hz, CH₃). ³¹P NMR (121 MHz, CDCl₃) δ = 63.65. IR $\nu_{\text{max}}/\text{cm}^{-1}$ 3056 w, 2955 m, 2853 w, 1673 m, 1615 w, 1602 w, 1472 m. HRMS (NESI): *m/z* calcd for C₄₇H₅₉Al₂OP₂S: 1127.3087 [M – SbF₆]⁺; found: 1127.3084.

Compound 6b. Complex **6b** was obtained as white crystals (8.4 mg, 0.0065 mmol, 97%). M.p. 184 °C (decomposes). ¹H NMR (300 MHz, CD₂Cl₂) δ 7.93–7.84 (m, 2H, Ar-H), 7.62–7.45 (m, 6H, Ar-H), 7.35–7.16 (m, 11H, Ar-H), 7.15–7.09 (m, 4H, Ar-H), 1.37 (d, *J*(¹H–³¹P) = 15.8 Hz, 36H, C(CH₃)₃). ¹³C NMR (75 MHz, CD₂Cl₂) δ 149.8 (d, *J*(¹³C–³¹P) = 14.2 Hz, C), 143.3 (d, *J*(¹³C–³¹P) = 6.7 Hz, C), 134.4 (CH), 133.73 (d, *J*(¹³C–³¹P) = 7.6 Hz, CH), 133.72 (CH), 131.7 (CH), 129.9 (CH), 129.7 (CH), 129.3 (CH), 129.2 (CH), 128.5 (CH), 128.1 (CH), 128.0 (CH), 127.8 (C), 127.5 (CH), 125.8 (d, *J*(¹³C–³¹P) = 44.3 Hz, C), 38.5 (d, *J*(¹³C–³¹P) = 23.7 Hz, C), 31.3 (d, *J*(¹³C–³¹P) = 6.9 Hz, CH₃). ³¹P NMR (121 MHz, CD₂Cl₂) δ 62.87. IR $\nu_{\text{max}}/\text{cm}^{-1}$ 2951 m, 2886 w, 1577 m, 1469 m, 1440 m. HRMS (NESI): *m/z* calcd for C₄₆H₅₉Al₂OP₂S: 1099.3138 [M – SbF₆]⁺; found: 1099.3137.

Compound 6c. Complex **6c** was obtained as yellow crystals (19.3 mg, 0.015 mmol, 55%). M.p. 193 °C; ¹H NMR (300 MHz, CDCl₃) δ = 7.94–7.83 (m, 2H, Ar-H), 7.61–7.09 (m, 16H, Ar-H), 2.65–2.50 (m, 2H, SCH₂), 1.56–1.25 (m, 4H, alkyl CH₂), 1.40 (d, *J* = 15.7, 36H, C(CH₃)₃), 0.84 (t, *J* = 7.3, 3H, CH₂CH₃). ¹³C NMR (100 MHz, CDCl₃) δ = 149.3 (d, *J*(¹³C–³¹P) = 14.2 Hz, C), 143.1 (d, *J*(¹³C–³¹P) = 6.7 Hz, C), 134.1 (CH), 133.3 (d, *J*(¹³C–³¹P) = 7.8 Hz, CH), 131.2 (CH), 129.6 (CH), 128.7 (CH), 128.0 (CH), 127.6 (d, *J*(¹³C–³¹P) = 6.9 Hz, CH), 125.8 (d, *J*(¹³C–³¹P) = 43.3 Hz, C), 40.1 (CH₂), 38.2 (d, *J*(¹³C–³¹P) = 23.5 Hz, C), 32.9

(CH₂), 31.0 (d, *J*(¹³C–³¹P) = 6.8 Hz, CH₃), 22.0 (CH₂), 13.9 (CH₃). ³¹P NMR (162 MHz, CDCl₃) δ = 62.75. IR $\nu_{\text{max}}/\text{cm}^{-1}$ 2956 m, 2901 w, 2872 w, 1462 m, 1441 m, 1430 m. HRMS (NESI): *m/z* calcd for C₄₄H₆₃Al₂OP₂S: 1079.3451 [M – SbF₆]⁺; found: 1079.3434.

Compound 7a. Complex **7a** was obtained as white crystals (21.0 mg, 0.025 mmol, 98%). M.p. 185 °C (decomposes). ¹H NMR (400 MHz, CDCl₃) δ = 7.85 (td, *J* = 7.9 Hz, 1.8, 1H, Ar-H), 7.65–7.51 (m, 5H, Ar-H), 7.34–7.24 (m, 5H, Ar-H), 7.20–7.12 (m, 1H, Ar-H), 7.01 (d, *J* = 7.6 Hz, 2H, Ar-H), 4.67 (br. s, 2H, NH₂), 1.36 (d, *J* = 16.1 Hz, 18H, C(CH₃)₃). ¹³C NMR (100 MHz, CDCl₃) δ = 149.1 (d, *J*(¹³C–³¹P) = 12.1 Hz, C), 144.0 (d, *J*(¹³C–³¹P) = 6.3 Hz, C), 133.4 (CH), 133.3 (d, *J*(¹³C–³¹P) = 10.1 Hz, CH), 131.5 (d, *J*(¹³C–³¹P) = 2.1 Hz, CH), 130.5 (CH), 129.8 (CH), 129.2 (CH), 127.6 (d, *J*(¹³C–³¹P) = 7.3 Hz, CH), 127.2 (CH), 126.3 (broad, C), 125.1 (d, *J*(¹³C–³¹P) = 48.5 Hz, C), 121.7 (broad, CH), 38.0 (d, *J*(¹³C–³¹P) = 26.2 Hz, C), 30.9 (d, *J*(¹³C–³¹P) = 6.1 Hz, CH₃). ³¹P NMR (162 MHz, CDCl₃) δ = 58.86. IR $\nu_{\text{max}}/\text{cm}^{-1}$ 3314 w, 3266 m, 3016 w, 2954 w, 1605 m, 1590 m, 1496 m, 1474 m, 1462 m. HRMS (NESI): *m/z* calcd for C₂₆H₃₄AlNP: 588.2089 [M – SbF₆]⁺; found: 588.2089. Anal. Calc. for C₂₆H₃₄AlF₆NPSb: C, 37.88; H, 4.17; N, 1.70. Found: C, 37.88; H, 4.13; N, 1.34.

Compound 7b. Complex **7b** was obtained as white crystals (22.1 mg, 0.026 mmol, 99%). M.p. 173 °C (decomposes). ¹H NMR (300 MHz, CDCl₃) δ = 7.90–7.81 (m, 1H, Ar-H), 7.63–7.50 (m, 4H, Ar-H), 7.36–7.22 (m, 4H, Ar-H), 6.96 (d, *J* = 8.9 Hz, 2H, Ar-H), 6.80 (d, *J* = 8.9 Hz, 2H, Ar-H), 4.57 (br s, 2H, NH₂), 3.78 (s, 3H, OCH₃), 1.38 (d, *J*(¹H–³¹P) = 16.1 Hz, 18H, C(CH₃)₃). ¹³C NMR (101 MHz, CDCl₃) δ = 157.7 (broad, C), 149.2 (d, *J*(¹³C–³¹P) = 12.5 Hz, C), 144.0 (d, *J*(¹³C–³¹P) = 6.5 Hz, C), 133.4 (d, *J*(¹³C–³¹P) = 6.0 Hz, CH), 133.3 (d, *J*(¹³C–³¹P) = 10.3 Hz, CH), 131.4 (d, *J*(¹³C–³¹P) = 2.2 Hz, CH), 130.5 (CH), 129.2 (CH), 127.6 (d, *J*(¹³C–³¹P) = 7.4 Hz, CH), 127.2 (CH), 125.1 (d, *J*(¹³C–³¹P) = 48.4 Hz, C), 123.1 (broad, C), 114.9 (CH), 114.9 (CH), 55.7 (CH₃), 38.0 (d, *J*(¹³C–³¹P) = 26.3 Hz, C), 30.9 (d, *J*(¹³C–³¹P) = 6.1 Hz, CH₃). ³¹P NMR (121 MHz, CDCl₃) δ = 58.71. IR $\nu_{\text{max}}/\text{cm}^{-1}$ 3312 w, 3268 w, 2960 w, 1607 w, 1577 m, 1510 s, 1458 m, 1245 s. HRMS (NESI): *m/z* calcd for C₂₇H₃₆AlNOP: 618.2195 [M – SbF₆]⁺; found: 618.2182. Anal. Calc. for C₂₇H₃₆AlF₆NOPSb: C, 37.96; H, 4.26; N, 1.64. Found: C, 37.76; H, 4.25; N, 1.52.

Compound 7c. Complex **7c** was obtained as white crystals (19.7 mg, 0.024 mmol, 94%). M.p. 173 °C (decomposes); ¹H NMR (300 MHz, CDCl₃) δ = 7.86 (td, *J* = 7.6, 1.7 Hz, 1H, Ar-H), 7.64–7.47 (m, 4H, Ar-H), 7.35–7.17 (m, 4H, Ar-H), 2.91–2.68 (m, 4H, NH₂CH₂), 1.54–1.23 (m, 22H, C(CH₃)₃ & CH₂CH₂CH₃), 0.90 (t, *J* = 7.3 Hz, 3H, CH₂CH₃). ¹³C NMR (100 MHz, CDCl₃) δ = 149.2 (d, *J*(¹³C–³¹P) = 12.7 Hz, C), 143.8 (d, *J*(¹³C–³¹P) = 6.6 Hz, C), 133.6 (d, *J*(¹³C–³¹P) = 3.2 Hz, CH), 133.3 (d, *J*(¹³C–³¹P) = 7.5 Hz, CH), 131.4 (d, *J*(¹³C–³¹P) = 2.1 Hz, CH), 130.3 (CH), 128.9 (CH), 127.6 (d, *J*(¹³C–³¹P) = 7.3 Hz, CH), 127.4 (CH), 125.3 (d, *J*(¹³C–³¹P) = 47.8 Hz, C), 45.5 (CH₂), 38.0 (d, *J*(¹³C–³¹P) = 26.3 Hz, C), 34.2 (CH₂), 30.9 (d, *J*(¹³C–³¹P) = 6.1 Hz, CH₃), 19.7 (CH₂), 13.8 (CH₃). ³¹P NMR (121 MHz, CDCl₃) δ = 58.30; IR $\nu_{\text{max}}/\text{cm}^{-1}$ 3320 m, 3276 m, 2962 m, 2902 w, 1474 s,



1461 s. HRMS (NESI): m/z calcd for $C_{24}H_{38}AuNP$: 568.2402 [$M - SbF_6^-$]⁺; found: 568.2399. Anal. Calc. for $C_{24}H_{38}AuF_6NPSb$: C, 35.84; H, 4.77; N, 1.74. Found: C, 36.13; H, 4.75; N, 1.49.

Crystal data

Single crystal X-ray diffraction data were collected on crystals **6a**, **6c**, **7a**–**c** which were coated in Paratone-N oil and mounted on an X8 Apex2 diffractometer with a MiTiGen

Micromount. Diffraction data were collected at 100 K with graphite monochromated MoK α radiation from a sealed X-ray tube set at 50 kV and 35 mA. Diffraction data for **6b** were collected on an Agilent SuperNova, Dual, Atlas diffractometer using Cu K α radiation (1.5418 Å) with mirror optics. The crystal was kept at 120.01(10) K during data collection. Using Olex2,²⁴ the structure was solved with the XS²⁵ structure solution program using Direct Methods and refined with the XL²⁵

Table 4 Crystal data and structure refinements for **6a**–**c** and **7a**–**c**

	6a	6b	6c
Empirical formula	$C_{47}H_{59}O_6P_2SSbAu_2$	$C_{46}H_{59}Au_2F_6P_2SSb$	$C_{44}H_{63}Au_2F_6P_2SSb \cdot 0.5(CHCl_3)$
Formula weight	1363.63	1335.61	1375.31
Temperature/K	100(2)	120.01(10)	100.15
Crystal system	Triclinic	Monoclinic	Monoclinic
Space group	$P\bar{1}$	Cc	$P2_1/n$
$a/\text{\AA}$	13.4006(7)	24.6918(3)	12.0540(8)
$b/\text{\AA}$	13.5192(7)	13.08924(15)	30.084(2)
$c/\text{\AA}$	15.7860(8)	29.3558(4)	13.5903(8)
$\alpha/^\circ$	68.403(2)	90.0	90.00
$\beta/^\circ$	80.115(2)	90.7654(11)	96.316(3)
$\gamma/^\circ$	65.851(2)	90.0	90.00
Volume/Å ³	2425.6(2)	9486.84(19)	4898.4(5)
Z	2	8	4
$\rho_{\text{calc}} \text{ mg mm}^{-3}$	1.867	1.870	1.865
m/mm^{-3}	6.752	17.388	6.765
$F(000)$	1316.0	5152.0	2660.0
Crystal size/mm ³	0.40 × 0.40 × 0.30	0.2426 × 0.123 × 0.056	0.38 × 0.32 × 0.28
2 θ range for data collection	2.78 to 52.74°	6.017 to 152.5034°	2.7 to 66.64°
Index ranges	$-16 \leq h \leq 16, -13 \leq k \leq 16, -18 \leq l \leq 19$	$-31 \leq h \leq 29, -16 \leq k \leq 15, -36 \leq l \leq 36$	$-18 \leq h \leq 18, -46 \leq k \leq 46, -20 \leq l \leq 20$
Reflections collected	35 962	77 919	136 649
Independent reflections	9865 [$R(\text{int}) = 0.0351$]	19 283 [$R(\text{int}) = 0.0447$]	18 698 [$R(\text{int}) = 0.0549$]
Data/restraints/parameters	9865/0/553	19 283/2/1069	18 698/13/600
Goodness-of-fit on F^2	1.139	1.041	1.081
Final R indexes [$I \geq 2\sigma(I)$]	$R_1 = 0.0216, wR_2 = 0.0545$	$R_1 = 0.0313, wR_2 = 0.0819$	$R_1 = 0.0328, wR_2 = 0.0713$
Final R indexes [all data]	$R_1 = 0.0259, wR_2 = 0.0707$	$R_1 = 0.0315, wR_2 = 0.0820$	$R_1 = 0.0468, wR_2 = 0.0765$
Largest diff. peak/hole/e Å ⁻³	0.99/−1.48	1.53/−0.91	4.07/−4.72
	7a	7b	7c
Empirical formula	$C_{26}H_{34}NF_6PSbAu$	$C_{27}H_{36}AuF_6NOPSb$	$C_{24}H_{38}AuF_6NPSb$
Formula weight	824.23	854.25	804.24
Temperature/K	100.15	100(2)	100(2)
Crystal system	Monoclinic	Monoclinic	Monoclinic
Space group	$P2_1/c$	$P2_1/c$	$P2_1/c$
$a/\text{\AA}$	7.5686(4)	13.1268(4)	7.6009(4)
$b/\text{\AA}$	17.4546(9)	11.7372(4)	17.7750(9)
$c/\text{\AA}$	20.8291(11)	19.9682(7)	20.5702(10)
$\alpha/^\circ$	90.00	90.00	90.00
$\beta/^\circ$	95.628(3)	106.108(2)	98.499(2)
$\gamma/^\circ$	90.00	90.00	90.00
Volume/Å ³	2738.4(2)	2955.75(17)	2748.6(2)
Z	4	4	4
$\rho_{\text{calc}} \text{ mg mm}^{-3}$	1.999	1.920	1.943
m/mm^{-3}	6.453	5.985	6.426
$F(000)$	1584.0	1648.0	1552.0
Crystal size/mm ³	0.43 × 0.38 × 0.26	0.22 × 0.12 × 0.08	0.4 × 0.38 × 0.04
2 θ range for data collection	4.58 to 72.04°	4.82 to 60.32°	3.04 to 70.38°
Index ranges	$-12 \leq h \leq 12, -28 \leq k \leq 28, -32 \leq l \leq 34$	$-18 \leq h \leq 17, 0 \leq k \leq 16, 0 \leq l \leq 28$	$-12 \leq h \leq 12, -27 \leq k \leq 28, -33 \leq l \leq 29$
Reflections collected	69 144	102 285	82 430
Independent reflections	12 891 [$R(\text{int}) = 0.0376$]	8722 [$R(\text{int}) = 0.0691$]	11 854 [$R(\text{int}) = 0.0375$]
Data/restraints/parameters	12 891/0/337	8722/2/359	11 854/6/349
Goodness-of-fit on F^2	1.024	1.029	1.026
Final R indexes [$I \geq 2\sigma(I)$]	$R_1 = 0.0235, wR_2 = 0.0458$	$R_1 = 0.0294, wR_2 = 0.0508$	$R_1 = 0.0285, wR_2 = 0.0639$
Final R indexes [all data]	$R_1 = 0.0324, wR_2 = 0.0480$	$R_1 = 0.0436, wR_2 = 0.0546$	$R_1 = 0.0466, wR_2 = 0.0691$
Largest diff. peak/hole/e Å ⁻³	3.29/−2.04	0.72/−1.03	1.76/−1.80



refinement package using least squares minimisation. All non hydrogen atoms were refined anisotropically. All H atoms including water were constrained to idealised geometries apart from N bound H atoms in **7a–7c**. CCDC 914704 (**6a**), 896069 (**6b**), 914705 (**6c**), 914706 (**7a**), 914707 (**7b**), and 914708 (**7c**), contain the supplementary crystallographic data for this paper (see Table 4 for crystal data and structure refinements).

General procedure for Table 1

A solution of thiophenol (1 equiv.) and catalyst (2.5 mol%) in CH_2Cl_2 (0.2 mL) was added to a solution of cyclopropene **11** (1 equiv.) in CH_2Cl_2 (0.52 mL) at 25 °C and stirred for 30 min. The solution was then filtered through a plug of silica with diethyl ether, and concentrated under reduced pressure. The reaction mixture was analysed by ^1H NMR in CDCl_3 to determine **12:13** ratio by comparison with literature known spectra.^{2f}

General procedure for Table 2

Catalyst (5 mol%) was added to a stirred solution of cyclopropene **14** (1.2 equiv.) and *p*-anisidine (1 equiv.) in CH_2Cl_2 (0.1 M). The resulting solution was stirred for 18 h at 25 °C, filtered through a silica plug with ether and concentrated under reduced pressure. The reaction mixture was then analysed by ^1H NMR in CDCl_3 to determine reaction conversion by comparison with literature known spectra.^{2f}

General procedure for Table 3

Catalyst (5 mol% with respect to gold) was added in one portion to a stirred solution of cyclopropene **11** (1 equiv.) and phenethyl alcohol (1 equiv.) in CH_2Cl_2 (0.48 M). The resulting solution was stirred for 19 h at 20 °C, the mixture was then filtered through a silica plug with ether and concentrated under reduced pressure. The reaction mixture was then analysed by ^1H NMR in CDCl_3 to determine reaction conversion by comparison with spectra of isolated **16** (see ESI†).

Acknowledgements

We thank EPSRC (PCY) for funding, EPSRC UK National Mass Spectrometry Facility at Swansea University for analytical services and Dr Scott J. Dalgarno and Dr Gary Nichol for additional single crystal X-ray crystallography.

Notes and references

- For selected reviews on gold catalysis, see: (a) A. Corma, A. Leyva-Peréz and M. J. Sabater, *Chem. Rev.*, 2011, **111**, 1657; (b) M. Bandini, *Chem. Soc. Rev.*, 2011, **40**, 1358; (c) T. C. Boorman and I. Larrosa, *Chem. Soc. Rev.*, 2011, **40**, 1910; (d) A. S. K. Hashmi and M. Bührle, *Aldrichimica Acta*, 2010, **43**, 27; (e) N. D. Shapiro and F. D. Toste, *Synlett*, 2010, 675; (f) S. Sengupta and X. Shi, *ChemCatChem*, 2010, **2**, 609; (g) N. Bongers and N. Krause, *Angew. Chem., Int.*

- Ed.*, 2008, **47**, 2178; (h) D. J. Gorin, B. D. Sherry and F. D. Toste, *Chem. Rev.*, 2008, **108**, 3351; (i) E. Jiménez-Núñez and A. M. Echavarren, *Chem. Rev.*, 2008, **108**, 3326; (j) Z. Li, C. Brouwer and C. He, *Chem. Rev.*, 2008, **108**, 3239; (k) A. Arcadi, *Chem. Rev.*, 2008, **108**, 3266; (l) J. Muzart, *Tetrahedron*, 2008, **64**, 5815; (m) A. S. K. Hashmi and M. Rudolph, *Chem. Soc. Rev.*, 2008, **37**, 1766; (n) H. C. Shen, *Tetrahedron*, 2008, **64**, 7847; (o) H. C. Shen, *Tetrahedron*, 2008, **64**, 3885; (p) R. A. Widenhoefer, *Chem.-Eur. J.*, 2008, **14**, 5382; (q) D. J. Gorin and F. D. Toste, *Nature*, 2007, **446**, 395; (r) A. Fürstner and P. W. Davies, *Angew. Chem., Int. Ed.*, 2007, **46**, 3410; (s) E. Jiménez-Núñez and A. M. Echavarren, *Chem. Commun.*, 2007, 333; (t) A. S. K. Hashmi, *Chem. Rev.*, 2007, **107**, 3180; (u) A. S. K. Hashmi and G. J. Hutchings, *Angew. Chem., Int. Ed.*, 2006, **45**, 7896; (v) M. Rudolph and A. S. K. Hashmi, *Chem. Soc. Rev.*, 2012, **41**, 2448.
- (a) J. T. Bauer, M. S. Hadfield and A. L. Lee, *Chem. Commun.*, 2008, 6405; (b) M. S. Hadfield, J. T. Bauer, P. E. Glen and A. L. Lee, *Org. Biomol. Chem.*, 2010, **8**, 4090; (c) M. S. Hadfield and A.-L. Lee, *Chem. Commun.*, 2011, **47**, 1333; (d) P. C. Young, M. S. Hadfield, L. Arrowsmith, K. M. Macleod, R. J. Mudd, J. A. Jordan-Hore and A.-L. Lee, *Org. Lett.*, 2012, **14**, 898; (e) M. S. Hadfield, L. J. Häller, A.-L. Lee, S. A. Macgregor, J. A. T. O'Neill and A. M. Watson, *Org. Biomol. Chem.*, 2012, **10**, 4433; (f) R. J. Mudd, P. C. Young, J. A. Jordan-Hore, G. M. Rosair and A.-L. Lee, *J. Org. Chem.*, 2012, **77**, 7633.
- For reviews on gold-catalysed reactions with cyclopropenes, see: (a) B.-L. Lu, L. Dai and M. Shi, *Chem. Soc. Rev.*, 2012, **41**, 3318; (b) F. Miege, C. Meyer and J. Cossy, *Beilstein J. Org. Chem.*, 2011, **7**, 717.
- (a) M. S. Hadfield and A. L. Lee, *Org. Lett.*, 2010, **12**, 484; (b) A. Heuer-Jungemann, R. G. McLaren, M. S. Hadfield and A.-L. Lee, *Tetrahedron*, 2011, **67**, 1609; (c) K. J. Kilpin, U. S. D. Paul, A. L. Lee and J. D. Crowley, *Chem. Commun.*, 2011, **47**, 328.
- P. C. Young, N. A. Schopf and A.-L. Lee, *Chem. Commun.*, 2013, **49**, 4262.
- (a) A. Ulman, *Chem. Rev.*, 1996, **96**, 1533; (b) H. Gronbeck, A. Curioni and W. J. Andreoni, *J. Am. Chem. Soc.*, 2000, **122**, 3839; (c) K. Fujita, N. Nakamura, H. Ohno, B. S. Leigh, K. Niki, H. B. Gray and J. H. J. Richards, *J. Am. Chem. Soc.*, 2004, **126**, 13954.
- Gold(i)-catalysed reactions with thiols are still relatively scarce, see for example: with allenes: (a) N. Morita and N. Krause, *Angew. Chem., Int. Ed.*, 2006, **45**, 1897; (b) M. N. Menggenbatee, G. Ferrara, N. Nishina, T. Jin and Y. Yamamoto, *Tetrahedron Lett.*, 2010, **51**, 4627. For mechanistic study, see: (c) K. Ando, *J. Org. Chem.*, 2010, **75**, 8516. With dienes: (d) C. Brouwer, R. Rahaman and C. He, *Synlett*, 2007, 1785. See also: (e) A. Arcadi, G. B. S. Di Giuseppe and F. Marinelli, *Green Chem.*, 2003, **5**, 64. Using heterogenised gold complexes: (f) A. Corma, C. González-Arellano, M. Iglesias and F. Sánchez, *Appl. Catal., A*, 2010, **375**, 49. For examples of other low-valent sulfur employed



as nucleophiles in gold-catalyzed reactions, see: (g) I. Nakamura, T. Sato and Y. Yamamoto, *Angew. Chem., Int. Ed.*, 2006, **45**, 4473; (h) L. Peng, X. Zhang, S. Zhang and J. Wang, *J. Org. Chem.*, 2007, **72**, 1192; (i) P. W. Davies and S. J.-C. Albrecht, *Chem. Commun.*, 2008, 238; (j) P. W. Davies and S. J.-C. Albrecht, *Synlett*, 2012, 70.

8 For a recent related NMR study of coordination chemistry of gold in solution, see: A. Zhdanko, M. Ströbele and M. E. Maier, *Chem.-Eur. J.*, 2012, **18**, 14732.

9 Isolation and characterisation of gold-alkyne,-allene and alkene complexes are more prevalent. For examples of isolation and characterisation of gold complexes with: enol ether: (a) Y. Zhu, C. S. Day and A. C. Jones, *Organometallics*, 2012, **31**, 7332; dienes: (b) R. A. Sanguramath, S. K. Patra, M. Green and C. A. Russell, *Chem. Commun.*, 2012, **48**, 1060; (c) R. A. Sanguramath, T. N. Hooper, C. P. Butts, M. Green, M. Green, J. E. McGrady and C. A. Russell, *Angew. Chem., Int. Ed.*, 2011, **50**, 7592; (d) R. E. M. Brooner and R. A. Widenhoefer, *Organometallics*, 2011, **30**, 3182; alkyne: (e) T. N. Hooper, M. Green and C. A. Russell, *Chem. Commun.*, 2010, **46**, 2313; alkene: (f) T. N. Hooper, M. Green, J. E. McGrady, J. R. Patel and C. A. Russell, *Chem. Commun.*, 2009, 3877; (g) R. E. M. Brooner and R. A. Widenhoefer, *Organometallics*, 2012, **31**, 768; T. J. Brown, M. G. Dickens and R. A. Widenhoefer, *Chem. Commun.*, 2009, 6451; (h) T. J. Brown, M. G. Dickens and R. A. Widenhoefer, *J. Am. Chem. Soc.*, 2009, **131**, 6350; allene: (i) T. J. Brown, A. Sugie, M. G. D. Leed and R. A. Widenhoefer, *Chem.-Eur. J.*, 2012, **18**, 6959–6971; (j) T. J. Brown, A. Sugie, M. G. Dickens and R. A. Widenhoefer, *Organometallics*, 2010, **29**, 4207.

10 The formation of $[\text{Lau}-\text{NH}_2\text{R}][\text{X}]$ species is perhaps the best studied of the two in terms of X-ray crystallographic structures, but as far as the authors are aware, there are no catalytic studies with these species, as these studies pre-date the explosion of interest in homogenous gold(i)-catalysis of the last decade. See: (a) J. Vicente, M. T. Chicote, R. Guerrero, I. M. Saura-Llamas, P. G. Jones and M. C. Ramírez de Arellano, *Chem.-Eur. J.*, 2001, **7**, 638; (b) K. Angermaier and H. Schmidbaur, *J. Chem. Soc., Dalton Trans.*, 1995, 559; (c) J. Vicente, M. T. Chicote, R. Guerrero and P. G. Jones, *J. Chem. Soc., Dalton Trans.*, 1995, 1251.

11 For a recent review on intermediates in gold catalysis, see: A. S. K. Hashmi, *Angew. Chem., Int. Ed.*, 2010, **49**, 5232.

12 The structure of complex **6b** has been disclosed while investigating gold-catalysed reactions with thiols (see ref. 2f). All other crystal structures and complexes isolated: **6a**, **6c**, **7a**, **7b** and **7c** are novel structures.

13 C. Nieto-Oberhuber, S. López, M. P. Muñoz, D. J. Cárdenas, E. Buñuel, C. Nevado and A. M. Echavarren, *Angew. Chem., Int. Ed.*, 2005, **44**, 6146.

14 For related crystal structures, see: (a) P. G. Jones and A. Weinkauf, *Z. Kristallogr.*, 1994, **209**, 87; (b) W. J. Hunks, M. C. Jennings and R. J. Puddephatt, *Inorg. Chem.*, 2000, **39**, 2699; (c) A. Sladek, K. Angermaier and H. Schmidbaur, *Chem. Commun.*, 1996, 1959.

15 For a review on aurophilic interactions, see: H. Schmidbaur and A. Schier, *Chem. Soc. Rev.*, 2012, **41**, 370.

16 (a) P. Pérez-Galán, N. Delpont, E. Herrero-Gómez, F. Maseras and A. M. Echavarren, *Chem.-Eur. J.*, 2010, **16**, 5324; (b) Q.-S. Li, C.-Q. Wan, R.-Y. Zou, F.-B. Xu, H.-B. Song, X.-J. Wan and Z.-Z. Zhang, *Inorg. Chem.*, 2006, **45**, 1888.

17 For related mechanistic studies of azaphilic versus carbophilic activation, see: J. J. Hirner, K. E. Roth, Y. Shi and S. A. Blum, *Organometallics*, 2012, **31**, 6843.

18 For comparison, Maier and co-workers have shown that the equilibrium lies substantially towards **10** in the presence of alcohols (see ref. 8). In the presence of water, Tang and Yu have reported a related study on (phosphine)gold(i) hydrates and their equilibria: Y. Tang and B. Yu, *RSC Adv.*, 2012, **2**, 12686.

19 Review: (a) A. Gómez-Suárez and S. P. Nolan, *Angew. Chem., Int. Ed.*, 2012, **51**, 8156. Selected papers: (b) D. Weber, T. D. Jones, L. L. Adduci and M. R. Gagné, *Angew. Chem., Int. Ed.*, 2012, **51**, 2452; (c) D. Weber, M. A. Tarselli and M. R. Gagné, *Angew. Chem., Int. Ed.*, 2009, **48**, 5733; (d) T. Brown, D. Weber, M. R. Gagné and R. A. Widenhoefer, *J. Am. Chem. Soc.*, 2012, **134**, 9134; (e) A. S. K. Hashmi, I. Braun, P. Nösel, J. Schädlich, M. Wieteck, M. Rudolph and F. Rominger, *Angew. Chem., Int. Ed.*, 2012, **51**, 4456; (f) J. E. Heckler, M. Zeller, A. D. Hunter and T. G. Gray, *Angew. Chem., Int. Ed.*, 2012, **51**, 5924.

20 For examples of related $[\text{Au}(\text{L})]_2(\mu\text{-OH})[\text{X}]$ complexes, see: (a) R. S. Ramón, S. Gaillard, A. Poater, L. Cavallo, A. M. Z. Slawin and S. P. Nolan, *Chem.-Eur. J.*, 2011, **17**, 1238; (b) S. Gaillard, J. Bosson, R. S. Ramón, P. Nun, A. M. Z. Slawin and S. P. Nolan, *Chem.-Eur. J.*, 2010, **16**, 13729 and ref. 8.

21 For other gold(i)-catalysed reactions with cyclopropenes, see ref. 2 and 3 and: (a) Z. B. Zhu and M. Shi, *Chem.-Eur. J.*, 2008, **14**, 10219; (b) C. K. Li, Y. Zeng and J. B. Wang, *Tetrahedron Lett.*, 2009, **50**, 2956; (c) C. K. Li, Y. Zeng, H. Zhang, J. Feng, Y. Zhang and J. B. Wang, *Angew. Chem., Int. Ed.*, 2010, **49**, 6413; (d) F. Miege, C. Meyer and J. Cossy, *Org. Lett.*, 2010, **12**, 4144; (e) E. Seraya, E. Slack, A. Ariafard, B. F. Yates and C. J. T. Hyland, *Org. Lett.*, 2010, **12**, 4768; (f) G. Seidel, R. Mynott and A. Fürstner, *Angew. Chem., Int. Ed.*, 2009, **48**, 2510; (g) D. Benitez, N. D. Shapiro, E. Tkatchouk, Y. Wang, W. A. Goddard III and F. D. Toste, *Nat. Chem.*, 2009, **1**, 482; (h) F. Miege, C. Meyer and J. Cossy, *Chem.-Eur. J.*, 2012, **18**, 7810.

22 Recent review on cyclopropene chemistry: Z.-B. Zhu, Y. Wei and Y. M. Shi, *Chem. Soc. Rev.*, 2011, **40**, 5534.

23 In related work, the formation of digold-phenylacetylene adducts from reacting **8** with phenylacetylene also liberates H^+ : A. Grirrane, H. Garcia, A. Corma and E. Álvarez, *ACS Catal.*, 2011, **1**, 1647.

24 O. V. Dolomanov, L. J. Bourhis, R. J. Gildea, J. A. K. Howard and H. Puschmann, *J. Appl. Crystallogr.*, 2009, **42**, 339.

25 G. M. Sheldrick, *Acta Crystallogr., Sect. A: Fundam. Crystallogr.*, 2008, **64**, 112.